

Effects of interdiffusion on the electronic properties of HgTe-CdTe superlattices

A. Simon, D. Bertho, D. Boiron, and C. Jouanin

Groupe d'Etude des Semiconducteurs, Université des Sciences et Techniques du Languedoc, place Bataillon, 34095 Montpellier CEDEX 5, France

(Received 22 February 1990)

The growth of HgTe-CdTe superlattices has shown the importance of the interdiffusion of constituent atoms across the interfaces of heterostructures. We study the effect of these processes on the electronic properties of these superlattices in the semiconducting regime using a multiband envelope-function approach. The influence of the strain resulting from the lattice mismatch for HgTe-CdTe superlattice growth on CdTe substrates is found to weakly modify the light-hole subbands while heavy-hole levels are lowered. The conduction and the light-hole subbands are found to have large amplitudes at the HgTe-CdTe interfaces. The evolution of the band gap as a function of the time during which interdiffusion occurs has been studied. This process widens the band gap, and its occurrence can explain the discrepancy between the measured values and those predicted by the theory, which are larger. The conduction subbands are pushed up in energy, while the hole subbands are lowered, and, for samples annealed for a long time, their energies reach limit values that correspond to the energy bands of the alloy folded into the superlattice period. The interfacial feature of conduction and light-hole states is very sensitive to the abrupt variation of the band edges near the interfaces. It is found that the interdiffusion process, which creates transition layers between the two semiconductor layers, leads to a disappearance of the localization near the interfaces. Our results indicate that there is already appreciable modification of the electronic properties for temperatures in the range of the superlattice growth temperature.

I. INTRODUCTION

Hg-Cd-Te alloys have been used for a long time as an active material for infrared devices and other electro-optical applications because their band gap is small and can be adjusted by changing composition. Recently, semiconductor quantum wells and superlattices composed of alternating HgTe and CdTe layers have been proposed as a novel and attractive manner to tailor material properties for given applications because of the ability to vary the superlattice band gap by modifications of parameters such as layer thicknesses.^{1,2} However, the fabrication of good-quality heterostructures with abrupt interfaces is especially needed in the more advanced devices. The growth of good crystalline-quality HgTe-CdTe superlattices using molecular-beam epitaxy has been achieved by several laboratories and has shown that a difficulty in obtaining these structures is due to the interdiffusion of constituent Hg, Cd, and Te atoms across the interfaces.³⁻⁵ Such interdiffusion influences the composition profile of the superlattice, which occurs during the growth and depends on the fabrication temperature and time. Moreover, the first generated layers are more modified than the last ones, and as a result, a spatial distribution of the layer thickness occurs.⁴ As the electronic and optical properties are strongly dependent on the well and barrier thicknesses, the interdiffusion processes are expected to lead to appreciable effects on electron and hole subbands and perhaps to change the level order. These effects will be particularly important concerning the properties which are related to abrupt variation of

the band edges at the interfaces. HgTe-CdTe superlattices have been predicted to have conduction- and light-hole-band wave functions with large amplitude at the interfaces,⁶⁻⁸ at least for $\mathbf{k}=0$. This is due to the continuity of the probability current at the interfaces, which means a change in the sign of the slope of the wave function because of the sign reversal of the bulk effective mass which results from the inverted position of these two bands in HgTe and CdTe. The wave function of these states localized near the interfaces are characterized by cusps, and their presence is related to the abrupt variation of the square-well potential in the region near the interface. The level features will be noticeably dependent on the interface quality.

Up to now, to our knowledge, there has been only one attempt to clarify the interdiffusion effect on the band gap of HgTe-CdTe superlattices.⁹ Within the framework of a two-band tight-binding model, the evolution of the band gap with respect to the width of the diffused region has been calculated and shrinkage of the HgTe layers by interdiffusion has been inferred to explain why the measured band gaps are larger than those predicted by theory.¹⁰ This analysis of results is based on a discontinuity of 40 meV between the valence-band maxima of HgTe and CdTe, which were deduced from the magneto-optical experiments¹¹ in agreement with the anion common rule. This estimation of the offset value has been recently reviewed, and a larger value, 350 meV, seem to explain better the different experimental data.¹²⁻¹⁵ A better knowledge of the effect of interdiffusion on the electronic properties of superlattices would be helpful in

order to predict their optical properties and know implications of interdiffusion on the optical devices. The purpose of this paper is to report the results of a detailed study on the electronic band structures of HgTe-CdTe superlattices and to obtain their evolution when interdiffusion is taken into account. In Sec. II, we describe the model used to describe the evolution of the composition profile during the growth of the heterostructure, and we briefly show how the envelope-function approach is used to obtain the energy bands when the composition profile varies. In Sec. III, results of calculations are given for several values of anneal time, and the effects of interdiffusion on the electronic states of superlattice are discussed.

II. METHOD AND MODEL

To determine the effects of interdiffusion on the composition profile, we use Fick's second diffusion law:

$$\frac{\partial C}{\partial t} = \frac{\partial}{\partial z} D \frac{\partial C}{\partial z}, \quad (1)$$

where $C(z, t)$ is the concentration in the growth direction [001]. For simplicity, the interdiffusion coefficient D is taken to be independent of the concentration. The solution of Eq. (1) can be obtained easily from the Fourier coefficients of the composition profile $C(K, t)$, which are given by

$$C(K, t) = C(K, 0) e^{-K^2 D t}. \quad (2)$$

For periodic structures like superlattices, only discrete values $K_n = 2\pi n/L$ are allowed, where L is the period of the modulation. We assume that at $t=0$, there is no diffusion and that the heterostructure is the periodic repetition of a HgTe layer with a width L_1 associated with a CdTe layer with a width $L_2 = L - L_1$ so that

$$C(z, 0) = 1, \quad -L_1/2 < z - nL < L_1/2$$

$$C(z, 0) = 0, \quad L_1/2 < z - nL < L - L_1/2.$$

In this case, the coefficients $C(K_n, 0)$ for $n \neq 0$ are given by

$$C(K_n, 0) = \frac{2}{\pi} \sin \left[\frac{\pi n L_1}{D} \right] \cos \left[\frac{2\pi z}{D} \right], \quad (3)$$

and $C(0, 0) = L_1/L$. From Eq. (2), one can see that $C(K, t)$ only depends on the product Dt . It varies also with the temperature and D changes significantly with T . Each Fourier coefficient $C(K, t)$ decreases exponentially with respect to time with a damping which increases as n^2 , and the composition profile of the HgTe-CdTe superlattice is altered appreciably at the growth temperature, the main contribution arising from first Fourier component. The interdiffusion effect transforms a superlattice formed by alternate layers of two pure superconductors well characterized, in a material with composition varying with the superlattice period between two extremes corresponding to two mixed semiconductors, the composition of which depends on the temperature and growth time. After a long time, the heterostructure be-

comes almost homogenized. From the composition profile, we can obtain the potential profile, assuming that the conduction- and valence-band edges depend linearly on the concentration of constituent atoms; physical parameters are also position dependent and can be obtained for each position by assuming that they are linearly dependent on the mercury concentration that we choose as a variable. For instance, the valence-band edge at the z position, where the concentration of mercury is x , is given by

$$E_v(z) = x E_v(\text{HgTe}) + (1-x) E_v(\text{CdTe}), \quad (4)$$

as it results from a linear interpolation between the values of pure materials. All the parameters which describe the properties of heterostructures with interdiffusion are also position dependent, and their variation must be taken into account.

The value of the valence-band offset in HgTe-CdTe superlattices has been the subject of controversy¹¹⁻¹⁵ and has provoked numerous band-structure studies in order to better understand the electronic properties of this material. Several methods can be used for such calculations. The tight-binding approximation¹⁶⁻¹⁹ is based on a complete description of the bulk electronic states, including the states of the whole of the Brillouin zone. This approach is necessary, for instance, when states far away from the zone center must be considered at the same time as those near the zone center as, for instance, in the case of an indirect band gap. Band-structure calculations have been also performed by a pseudopotential approach which includes extended states in \mathbf{k} space.²⁰ A third method which has been widely used in the calculation of the heterostructure electronic states is the envelope-function approximation, which is derived from $\mathbf{k}\cdot\mathbf{p}$ method, and to assume that the band structure of bulk material is well described by the Hamiltonian at the center of the Brillouin zone.²¹⁻²⁷ This method is the easier to implement, and a number of procedures have been proposed to carry out calculations, results obtained by the fact that the different ways are relatively independent of the calculation method. As we are only interested in the superlattice states near the zone center, we have chosen the envelope-function approach, and we shall concentrate our study on the states lying near the superlattice band gap in a limited energy range. We assume that the electronic band structure of the two bulk materials which constitute the superlattice are well described by the Kane six-band model which includes the states with Γ_6 and Γ_8 symmetries. The Γ_7 states at the maximum of the split-off lie 1 eV below these states are not included in our basis. The interesting feature of the HgTe-CdTe heterostructure is due to the fact that HgTe is a zero-gap semiconductor. The Γ_8 degenerate state is both the conduction band and the heavy-hole band, while the Γ_6 state which lies below the Γ_8 state corresponds to the light-hole band. For CdTe, the level ordering is that usually found near the band gap for most semiconductors. The maximum of the valence band is a Γ_8 -symmetry state, and the minimum of the conduction band is a Γ_6 -symmetry state. The main consequence of this

configuration is the existence of bound states at the interfaces due to the abrupt change in the sign of the effective mass of the Γ_8 light-hole carriers, which produces a change in the sign of the slope of the wave function because of the continuity of the probability current. The same situation exists for Γ_6 -symmetry states. We study a superlattice grown along the [001] direction. The effective-mass Hamiltonian describing the Γ_6 and Γ_8 bands is a 6×6 matrix operator, quadratic in \mathbf{k} , given in atomic units by

$$H = \begin{pmatrix} E_e & 0 & i\sqrt{3}H_+ & \sqrt{2}H_z & iH_- & 0 \\ E_e & 0 & iH_+ & \sqrt{2}H_z & i\sqrt{3}H_- & 0 \\ & E_{hh} & A & C & 0 & 0 \\ & & E_{lh} & 0 & C & 0 \\ & & & E_{lh} & -A & 0 \\ & & & & & E_{hh} \end{pmatrix}, \quad (5)$$

where the terms relative to the valence band are

$$\begin{aligned} E_e &= E_{\Gamma_6} + \frac{1}{2}\gamma_0 k^2, \\ E_{hh} &= E_{\Gamma_8} - \frac{1}{2}(\gamma_1 \pm \gamma_2)k_x^2 - \frac{1}{2}(\gamma_1 \mp 2\gamma_2)k_z^2, \\ A &= i\sqrt{3}\gamma_3 k_- k_z, \\ C &= \frac{-\sqrt{3}}{2}[\gamma_2(k_x^2 - k_y^2) - 2i\gamma_3 k_x k_y]. \end{aligned}$$

The coupling between the conduction and valence states is described by

$$\begin{aligned} \sqrt{3}H_\alpha &= Pk_\alpha \quad (\alpha = x, y, z), \\ H_\pm &= \frac{1}{\sqrt{2}}(H_x \pm iH_y), \end{aligned}$$

where the interband momentum matrix element P is

$$P = -i \langle s | p_\alpha | \alpha \rangle.$$

In this equation, the Luttinger parameters γ_0 , γ_1 , γ_2 , and γ_3 , the interband momentum matrix element P , and the values of the conduction- and valence-band edges at $\mathbf{k}=\mathbf{0}$ are position dependent, and the matrix elements have been symmetrized to ensure the Hamiltonian hermiticity. Their variation in function of the position is assumed to be given by similar relations to Eq. (3). All the eigenvalues of this Hamiltonian are twofold degenerate because of the neglect of terms linear in k vectors which are present for materials crystallizing in the zinc-blende structure. Moreover, the directional dependence of subband dispersion in the k_x - k_y plane is assumed weak, and we adopt the axial approximation in replacing γ_2 and γ_3 by their average. In the envelope-function approximation, the electronic wave function $\Psi(\mathbf{k}, \mathbf{r})$ can be written in the form

$$\Psi(\mathbf{k}, \mathbf{r}) = \sum_j F_j(\mathbf{k}, \mathbf{r}) u_j^0(\mathbf{r}), \quad (6)$$

where $F_j(\mathbf{k}, \mathbf{r})$ is a six-component envelope function and the $u_j^0(\mathbf{r})$ are the periodic part of the Bloch functions for

the different spin states at $\mathbf{k}=\mathbf{0}$. For a superlattice, $\Psi(\mathbf{k}, \mathbf{r})$ must satisfy the Bloch theorem in the three directions and takes the form

$$F_j(\mathbf{k}, \mathbf{r}) = e^{i(k_x x + k_y y)} e^{ik_z z} f_j(z). \quad (7)$$

In comparison with the bulk, k_x and k_y remain good quantum numbers in the direction parallel to the interfaces, while k_z is now associated to the superlattice period L and $f_j(z)$ is a periodic function with the superlattice period. To obtain the envelope function and subband structure, the Schrödinger equation associated with the above Hamiltonian can be resolved in a variational scheme using a Fourier expansion as

$$f_j(z) = \sum_m c_{j,m} e^{2i\pi m z / L}. \quad (8)$$

As the lattice constant of HgTe is smaller than that of CdTe, internal strains are present, and a strain energy must be added to the Luttinger Hamiltonian. For superlattices grown on the CdTe substrate, the strain resulting from the mismatch is accommodated entirely in the HgTe layers which are stretched in x and y directions. This biaxial tensile stress is equivalent to both a hydrostatic dilatation, which reduces the band gap, and a uniaxial compression normal to the interfaces, which raises the light-hole bands compared to the heavy-hole bands. A reversal of the order in energy can result for the superlattice in the case where two bands are near each other.

III. RESULTS AND DISCUSSION

We have calculated the electronic structures along the two directions, [100] and [001], for an 8.2-nm-period HgTe-CdTe superlattice made up of two layers with equal thickness. These values have been chosen because experimental study on such a sample has been reported recently.⁵ The value of the parameters necessary for calculations as Luttinger parameters²³ and elastic constants²⁶ are reproduced in Table I. For the valence-band offset, we have adopted 350 meV, which is consistent with whole experimental data.¹² The first 13 terms are included in the Fourier expansion of the envelope function [Eq. (8)], which is really enough to obtain the energy bands with satisfactory precision. Figures 1(a) and 1(b) show the four subbands which are in the vicinity of the band gap for a HgTe-CdTe superlattice made up of two layers with equal thickness 4.1 nm. The subbands are calculated for the strained and unstrained cases. For these thicknesses, the HgTe-CdTe superlattice is a semiconductor with a direct band gap, and the highest band shown is the first conduction band. Because the heavy holes are not interacting with other subbands in the k_z direction, the H_1 and H_2 subbands present a weak dispersion, while interactions give a strong repulsion between subbands along the k_x direction. In particular, H_2 has an electronlike effective mass, and an anticrossing behavior arises from the repulsion between hole levels. The presence of a lattice mismatch of 0.3% entails a stress of 13 kbar on the HgTe layer. In bulk crystal, for the same stress, the hydrostatic dilatation reduces the band gap by

TABLE I. Luttinger parameters and elastic constants for HgTe and CdTe.

| | | | |
|---|-----------------------|--------|--------|
| Luttinger parameters (a.u.) | γ_0 | 1.0 | 1.0 |
| | γ_1 | 4.367 | 1.54 |
| | $\gamma_2 = \gamma_3$ | 1.034 | 0.015 |
| Momentum matrix element (eV) | P | 18 | 18 |
| Compliance constants (10^{-6} bar^{-1}) | S_{11} | 0.40 | 3.58 |
| | S_{12} | -0.16 | -1.39 |
| Deformation potentials (eV) | a | 3.8 | -2.74 |
| | b | -1.5 | -0.95 |
| Lattice constant (nm) | a_0 | 0.6462 | 0.6482 |

8 meV, while the uniaxial compression along [001] split the degeneracy between the heavy and light holes by 11 meV. As a result, the energy of the light hole is weakly increased by 3 meV; that of the heavy hole decreases by a

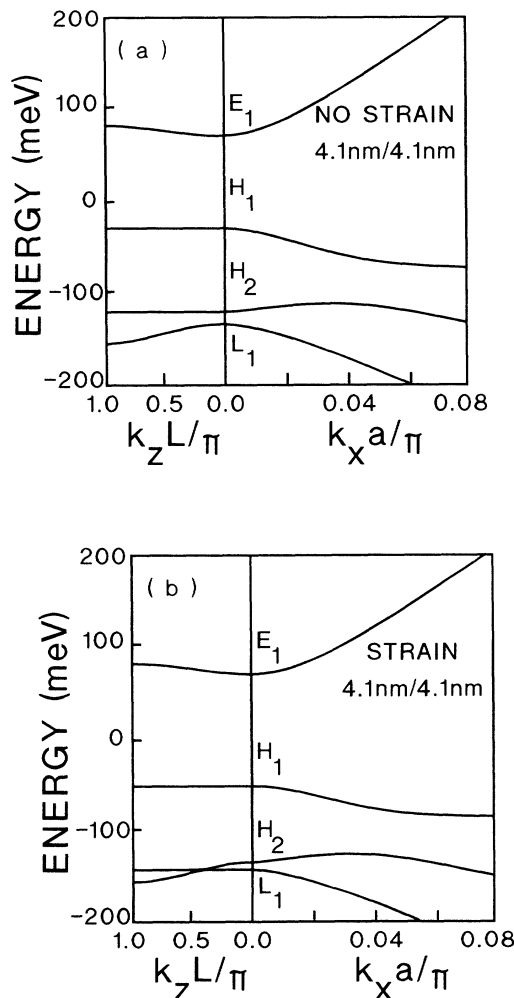


FIG. 1. Dispersion of the nearest subbands of the band gap in a HgTe-CdTe superlattice with two equal layers with thickness of 4.1 nm. (a) Without strain. (b) With strain.

more important amount of 19 meV, giving 22 meV for the splitting between the two kinds of holes. For the sample considered here, the superlattice band gap, which is the separation between E_1 and H_1 , is increased by the strain and its value which is 100 meV, neglecting the strain, becomes equal to 121 meV when strain effects are included. The energy variation is nearly the same as in the bulk semiconductor and is in agreement with results of Ref. 16. The order between H_2 and L_1 levels at the zone center is reversed by the strain, the heavy-hole band being pushed down in energy. Away from the zone center, strain effects are nearly the same as at Γ and the strain effect on the subband dispersion is an overall lowering of the heavy-hole subbands, the light-hole states being little affected. The main feature in the subband dispersion is the crossing of the L_1 and H_2 states, which appears in the k_z direction, while in the direction k_x , the bands cannot cross and repel. As quoted above, the states labeled E_1 and L_1 are expected to have large amplitude at the interfaces, at least near the zone center, because of the opposite sign of the effective mass of the electron and light hole in the two bulk materials. In Fig. 2(a), we give the envelope functions for the E_1 , H_1 , L_1 , and H_2 levels at Γ for the unstrained case. As expected, all these states are mainly confined to the HgTe layer

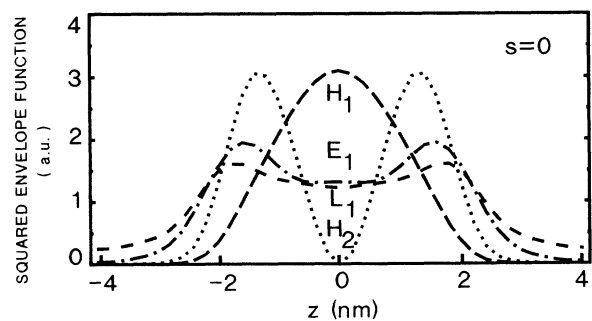


FIG. 2. Squared envelope functions for the Γ states near the band gap for a (4.1 nm)/(4.1 nm) HgTe-CdTe superlattice without interdiffusion. One unit supercell is shown, and the HgTe layer extends from -2.05 to 2.05 nm.

with some penetration in the barrier for the excited states. It can be seen that E_1 and L_1 states have a maximum amplitude at the interfaces between the two semiconductors, this feature being more accentuated for the electron state E_1 than for the light-hole state L_1 . The difference between the offset values for the two kinds of states provides a simple explanation of this situation. The absolute value of the bulk effective mass for E_1 and L_1 are nearly the same, but the offset values for the two kinds of states are very different, 1552 meV for conduction states and 350 meV for valence states. Thus the envelope function of the E_1 state decreases more rapidly than the L_1 one, giving a more abrupt feature, and the light-hole envelope function has a larger penetration in the barrier, which allows tunneling of light holes.

We now study the evolution of electronic properties when the interdiffusion process is considered, the strain effect being not included. Figure 3 shows the variation of the states at the center of the Brillouin zone as a function of the parameter $s = Dt$, which is proportional to the interdiffusion time. For the diffusion coefficient, we have used the phenomenological value $D = 4.2 \times 10^{-22} \text{ m}^2 \text{ s}^{-1}$, which has been deduced from x-ray analysis of HgTe-CdTe superlattices annealed at 185°C by a linear diffusion model.⁵ This value corresponds to an intermediate value of the interdiffusion coefficient for the HgTe and CdTe semiconductors. The interdiffusion process increases the energy of electron states E_1 , while it decreases the energy of the heavy and light holes H_1 , H_2 , and L_1 with a more pronounced effect for the H_1 and H_2 states. For samples annealed during a long time, the in-

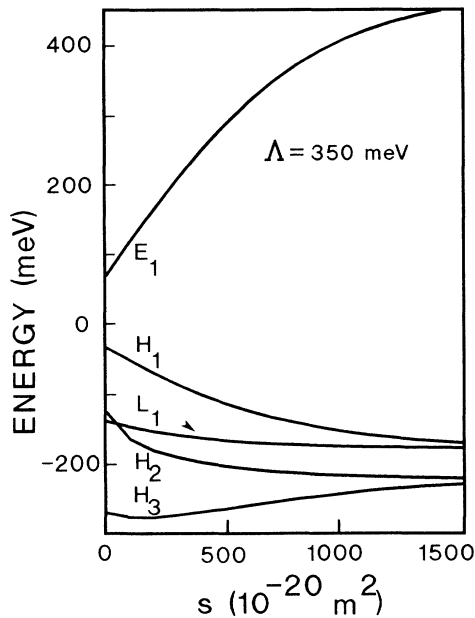


FIG. 3. Band-edge energies at Γ as a function of s , which is the product of the interdiffusion time by the diffusion coefficient, for a (4.1 nm)/(4.1 nm) superlattice.

terpenetration of the two semiconductors is large and the energies reach limit values which correspond to the conduction- and valence-band edges in the $\text{Hg}_{0.5}\text{Cd}_{0.5}\text{Te}$ alloy. These can be obtained as the means of the band edges of semiconductors. However, our calculations are carried out at the center of the Brillouin zone of the superlattice, and this value for the wave vector corresponds to the whole of the states in the Brillouin zone of the alloy with a wave vector multiple of $2\pi/L$. Limit values for valence-band energies begin to appear for $s = 1500 \times 10^{-20} \text{ m}^2$; they correspond to the states $k_z = 0, 2\pi/L$, and $4\pi/L$ of the Brillouin zone of the primitive lattice. The limit energy of H_1 and L_1 states is that of the valence-band edge of the alloy, while the H_2 and H_3 states have, respectively, the same energy as the heavy-hole bands for $k = 2\pi/L$ and $4\pi/L$ in the Δ direction. The band gap of the superlattice is increased by the interdiffusion as shown in Fig. 4 and is always larger than the band gap obtained without interdiffusion for abrupt band-edge profiles. This variation is nearly linear for interdiffusion time lower than about 2 h corresponding to $s = 200 \times 10^{-20} \text{ m}^2$ and the curve shows that for a superlattice kept for about 20 min at 185°C ($s = 50 \times 10^{-20} \text{ m}^2$), the band gap is increased by 50%, going from 102 to 143 meV. Such values for time and temperature correspond to about 0.7 nm of interdiffusion for atoms. This effect is very important for such a short time, and the interdiffusion strongly influences the band-gap value for the growth time generally used. This modification is mainly dependent on the value of the diffusion coefficient, which is difficult to know accurately because it depends on both the temperature and composition and, therefore, on the position in the material. In our calculation, the changes of D with the composition are not taken into account and only a mean value is used. This does not allow us to give prominence to the asymmetry of the well due to the different penetration of each component in the oth-

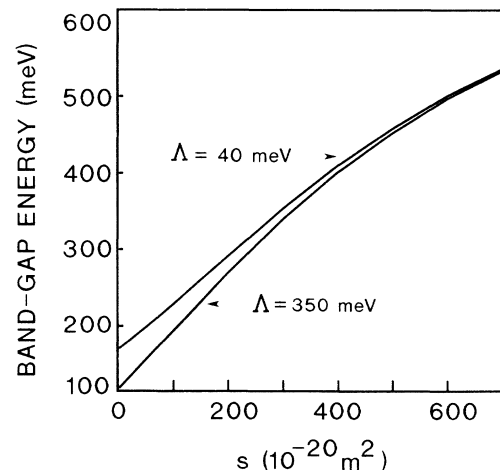


FIG. 4. Band gap E_g as a function of s for two values of the valence-band offset $\Delta = 40$ and 350 meV.

er, the Cd atoms penetrating more easily into the HgTe wells from the Hg atoms into CdTe barriers.⁴ However, the effects associated with the lack of the symmetry inversion are weak, and the electronic properties are more sensitive to other growth parameters like, in particular, the growth temperature. The interdiffusion coefficient varies about 2 or 3 orders of magnitude per 100 °C. For a growth temperature of 162 °C, the interdiffusion coefficient is $D = 1.23 \times 10^{-22} \text{ m}^2$,⁵ and for an interdiffusion time of 20 min, the band gap is 116 meV, to be compared to 143 meV obtained for 185 °C. The influence of the growth temperature is important and shows the relevance of reducing the processing temperature to obtain samples with a band gap which is not too dependent on the interdiffusion phenomena. The broadening of the band gap originating from the diffusion supplies an explanation to the fact that the measured band gap of superlattices appears to be larger than those predicted by the theory.¹⁰ The value of the valence-band offset in the HgTe-CdTe superlattice has been the subject of many discussions, and some values differing from $\Lambda = 350 \text{ meV}$ have been proposed. We have studied the effect of the interdiffusion on the superlattice band gap if another value $\Lambda = 40 \text{ meV}$ is used. The variation of the band gap can be compared in Fig. 4 with the curve obtained for $\Lambda = 350 \text{ meV}$, all the other parameters being the same. Also, in this case, the variation is linear up to $s = 300 \times 10^{-20} \text{ m}^2$, and the difference between the band gap calculated for the two offset values decreases with the interdiffusion time. However, the variation of superlattice states is different. For $\Lambda = 40 \text{ meV}$, the potential well seen by holes is small, and the confinement energies of the holes are weak and depend little on the potential profile. On the other hand, the conduction-band offset is large, and the evolution of the band gap is mainly due to the variation of the electron states which are strongly confined in HgTe layers and therefore more sensitive to the variation of the potential originating from the diffusion and to the presence of transition layers near the interfaces.

The localization of electron and light-hole states at the interfaces is due to the abrupt change in the sign of the effective mass across the interfaces. The interdiffusion modifies interfaces significantly, and we have studied the evolution of these states as a function of the interdiffusion time. Figure 5 shows the envelope function for the energy bands nearest the band gap for (4.1 nm)/(4.1 nm) samples annealed during progressive time. The envelope function of the heavy-hole state H_1 is only slightly modified for short periods of time. For a long annealing period, the offset value become weaker, the holes are more delocalized, and they penetrate more deeply into the barrier, while the maximum amplitude of the envelope function decreases. For a very long time, this function is constant because homogenization of the material is complete, giving the $\text{Hg}_{0.5}\text{Cd}_{0.5}\text{Te}$ alloy. The behavior of H_2 states is different. As for H_1 states, the lowering of the barrier potential increases their delocalization into the barrier. However, the H_2 envelope function is not constant for large interdiffusion time. In the completely homogenized material, the period of the su-

perlattice L produces a folding of the energy bands, and the H_2 states originate from the heavy-hole band in the bulk alloy along the [001] direction for the value $k_z = 2\pi/L$. The period of the wave function for this bulk state is L , and that of its square is $L/2$. This can be ob-

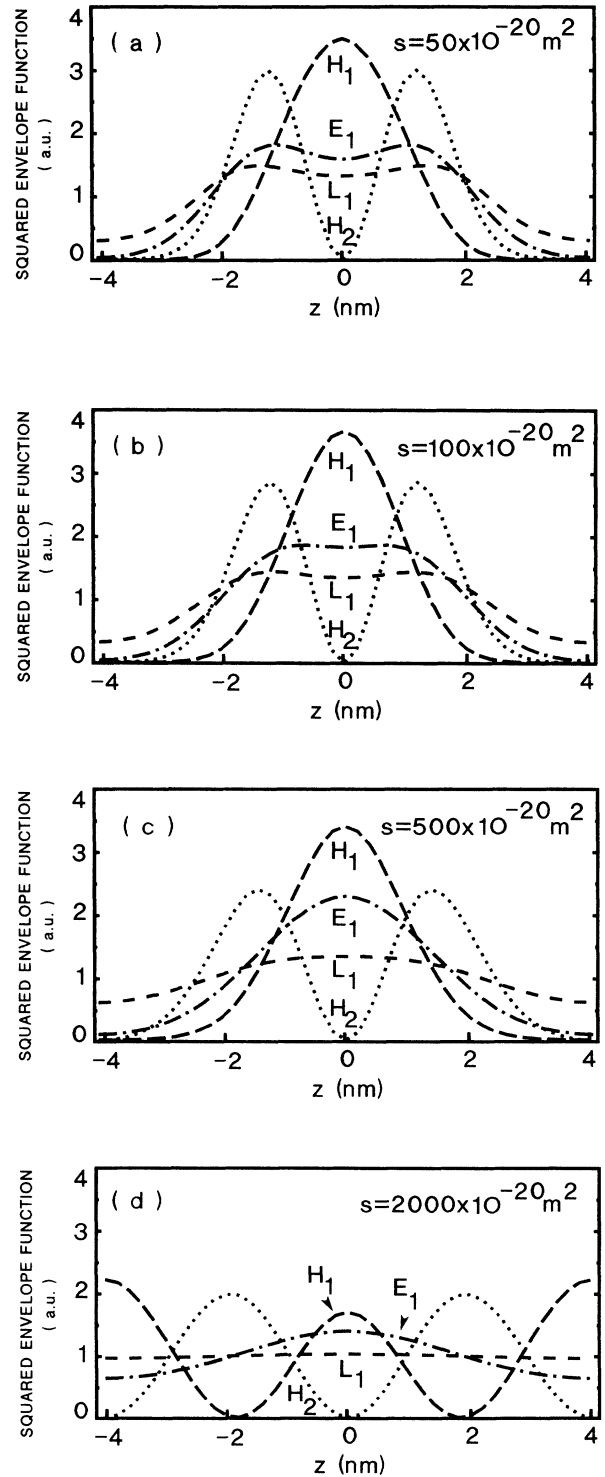


FIG. 5. Same as Fig. 2 for different s values: 50, 100, 500, and $2000 \times 10^{-20} \text{ m}^2$.

served in Fig. 5(d), which shows that the H_2 envelope function is odd and is a sinusoid with a period equal to half of the superlattice period. We have found that the E_1 and L_1 states are localized near the interfaces for $s=0$; this particular feature disappears when the atoms diffuse into the superlattice. The peaks at the interfaces have almost vanished for $s=10^{-18}$ m², which corresponds to annealing during a period of 40 min at 185 °C. With increasing interdiffusion time, E_1 and L_1 states become more extended into the barrier, this effect being larger for the L_1 state because the well potential is weaker than for the E_1 state. The sharp character of these states is strongly related to the presence of a transition zone between the two semiconductor layers, in which inversion of the slope of the envelope function occurs when going from HgTe to CdTe. As this zone widens when the interdiffusion time increases, the slope variation can be accommodated more gradually on a larger range, and the cusps on envelope functions soften and then disappear.

Until now, we have only considered heterostructures with barriers formed of pure CdTe before the interdiffusion process takes place. Since molecular-beam epitaxial growth produces barriers with a concentration of 15 at. % Hg, we investigate how the presence of some Hg in nominally CdTe barriers modifies our results. Initially, before the interdiffusion, the interfaces are abrupt, and we can suppose that the band offsets vary linearly with the Hg concentration. This entails a lowering of the valence- and conduction-band offsets of 15%, and the confinement effect by the HgTe wells could be less important. In fact, this effect can be neglected for the heavy holes because of their large effective mass, and it is not significant, a few meV, for the light holes. The conduction state is more sensitive to the offset variation, and the lower state has the same relative variation as the offset has. With an increase in the Hg content in the barrier, the superlattice band gap decreases until the conduction and H_1 bands just touch for about $x=0.6$. Then the superlattice becomes semimetallic. When interdiffusion takes place, the evolution of the band gap with time has the same behavior as for pure CdTe barriers with a slightly less abrupt variation. Such a feature can be

readily understood by referring to the situation for large interdiffusion time. Then the superlattice is equivalent to a homogeneous alloy of two semiconductors. If some Hg is present in the barrier before the interdiffusion, the Hg concentration in the final alloy is larger than for pure CdTe barriers and the limit gap value weaker.

IV. CONCLUSIONS

A variational multiband envelope-function method has been used to calculate the energy subband dispersion of HgTe-CdTe superlattices in order to investigate the effects of interdiffusion of constituent atoms across the interfaces of the heterostructure. The band structure of the semiconducting superlattice studied here is found not to be significantly influenced by the strain due to the lattice mismatch between HgTe-CdTe lattice constant, except for the band gap which widens without the energy bands being much distorted. The interdiffusion process is found to strongly affect the electronic properties of the superlattice. It increases the energy of the conduction state and lowers the heavy- and light-hole states, leading to a widening of the band gap during the time in which the interdiffusion takes place. This effect depends significantly on the temperature, and our calculations indicate appreciable broadening of the band gap for temperatures near the growth temperature used in molecular-beam epitaxy. This effect can explain the discrepancy that the measured gaps are larger than those predicted by the theory. The strong interfacial behavior of the conduction and light-hole states is smoothed by the occurrence of transition layers near the interfaces and completely disappears for larger interdiffusion time.

ACKNOWLEDGMENTS

The "Groupe d'Etude des Semiconducteurs" is a laboratory associated with the "Centre National de la Recherche Scientifique (Unité Recherche Associée No. 357)." The numerical results were obtained through the facilities of the Centre National Universitaire Sud de Calcul within the Centre de Compétence en Calcul Numérique Intensif operation.

- ¹J. N. Schulman and T. C. McGill, Appl. Phys. Lett. **34**, 663 (1979).
- ²D. L. Smith, T. C. McGill, and J. N. Schulman, Appl. Phys. Lett. **43**, 180 (1983).
- ³J. P. Faurie, A. Millon, and J. Piagnet, Appl. Phys. Lett. **41**, 713 (1982).
- ⁴K. Zanio and T. Massopust, J. Electron. Mater. **15**, 103 (1986); K. Zanio, J. Vac. Sci. Technol. A **4**, 2106 (1986).
- ⁵D. K. Arch, J. P. Faurie, J.-L. Staudenmann, M. Hibbs-Brenner, and P. Chow, J. Vac. Sci. Technol. **4**, 2101 (1986).
- ⁶Y. C. Chang, J. N. Schulman, G. Bastard, Y. Guldner, and M. Voos, Phys. Rev. B **31**, 2557 (1985).
- ⁷Y. R. Lin Liu and L. J. Sham, Phys. Rev. B **32**, 5561 (1985).
- ⁸N. A. Cade, J. Phys. C **18**, 5135 (1985).
- ⁹J. N. Schulman and Y. C. Chang, Appl. Phys. Lett. **46**, 571 (1985).
- ¹⁰J. P. Faurie, M. Boukerche, S. Sivanatan, J. Reno, and C. Hsu, Superlatt. Microstruct. **1**, 237 (1985).
- ¹¹Y. Guldner, G. Bastard, J. P. Vieren, M. Voos, J. P. Faurie, and A. Millon, Phys. Rev. Lett. **51**, 907 (1983).
- ¹²N. F. Johnson, P. M. Hui, and H. Ehrenreich, Phys. Rev. Lett. **61**, 1993 (1988); P. M. Hui, H. Ehrenreich, and N. F. Johnson, J. Vac. Sci. Technol. A **7**, 424 (1989).
- ¹³S. P. Kowalczyk, J. T. Cheung, E. A. Kraut, and R. W. Grant, Phys. Rev. Lett. **56**, 1605 (1986).
- ¹⁴T. M. Duc, C. Hsu, and J. P. Faurie, Phys. Rev. Lett. **58**, 1127 (1987).
- ¹⁵C. K. Shih and W. E. Spicer, Phys. Rev. Lett. **58**, 2594 (1987).
- ¹⁶J. N. Schulman and Y. C. Chang, Phys. Rev. B **33**, 2594 (1986).
- ¹⁷J. R. Meyer, F. J. Bartoli, C. A. Hoffman, and J. N. Schulman, Phys. Rev. B **38**, 12457 (1988).

- ¹⁸C. A. Hoffman, J. R. Meyer, F. J. Bartoli, J. W. Han, J. W. Cook, Jr., J. F. Schetzina, and J. N. Schulman, *Phys. Rev. B* **39**, 5208 (1989).
- ¹⁹M. Ritze and R. Enderlein, *J. Cryst. Growth* **101**, 359 (1990).
- ²⁰A. Zoryk and M. Jaros, *Appl. Phys. Lett.* **50**, 1191 (1987).
- ²¹G. Bastard, *Phys. Rev. B* **25**, 7584 (1982).
- ²²M. Altarelli, *Phys. Rev. B* **28**, 842 (1983).
- ²³J. M. Berroir, Y. Guldner, J. P. Vieren, M. Voos, and J. P. Faurie, *Phys. Rev. B* **34**, 891 (1986).
- ²⁴L. R. Ram-Mohan, K. H. Yoo, and R. L. Aggarwal, *Phys. Rev. B* **38**, 6151 (1988).
- ²⁵K. H. Yoo, R. L. Aggarwal, and L. R. Ram-Mohan, *J. Vac. Sci. Technol. A* **7**, 415 (1989).
- ²⁶G. Y. Wu and T. C. McGill, *Appl. Phys. Lett.* **47**, 634 (1985).
- ²⁷G. Y. Wu and T. C. McGill, *J. Appl. Phys.* **58**, 3914 (1985).